Supplementary Information

'Silver disposition and dynamics during electroless metal thin film synthesis'

Gyoung-Gug Jang,[a] *Michael Hawkridge*[b] *and D. Keith Roper*[a]*

[a] *Ralph E. Martin Department of Chemical Engineering, 3202 Bell Engineering Center, University of Arkansas, AR 72701*

[b] *Arkansas Material Characterization Facility, Institute of Nanoscience and Engineering, 731W Dickson St. University of Arkansas, AR 72701*

*To whom correspondence should be addressed. Tel: +1 479 575 6691. Fax: +1 479 575 7926.

E-mail: dkroper@uark.edu

Table of Contents

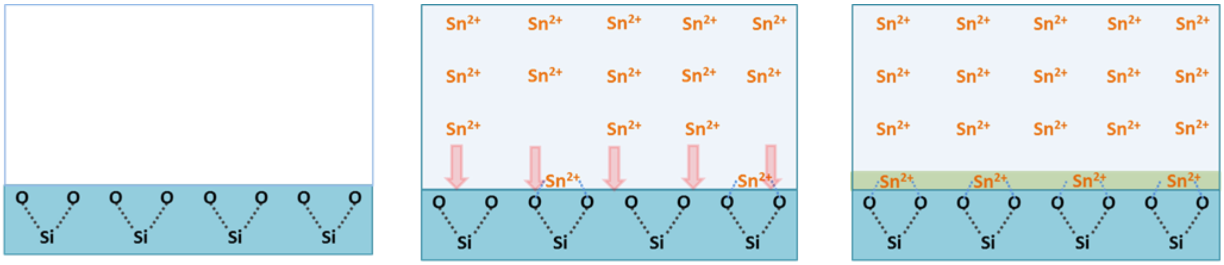

(1) Bare glass (2) Intro. Sn sol. (3) Sn sensitization

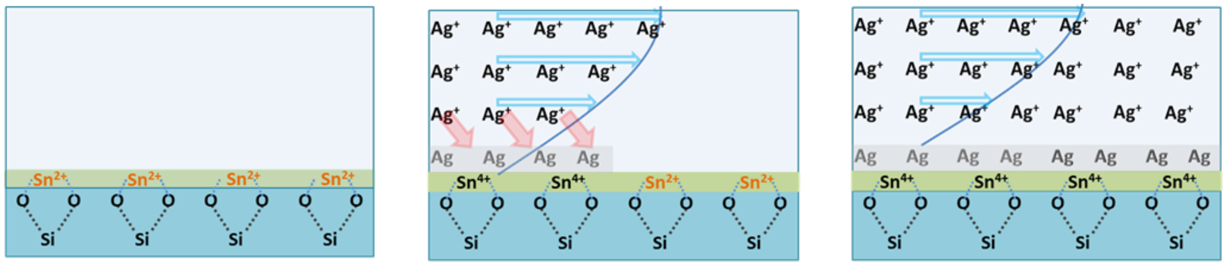

(4) H_2O washing (5) Intro. Ag sol. (6) Self limited Ag activation*

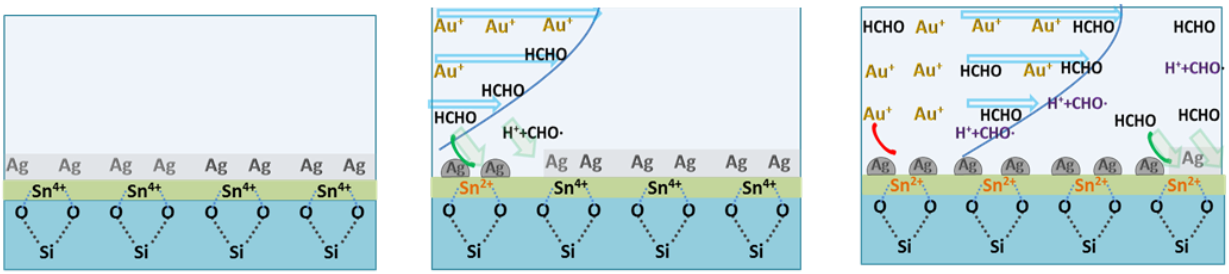

(7) H_2O washing (8) Intro. Au(I) +HCHO sol. (9) Instant Ag NP form*

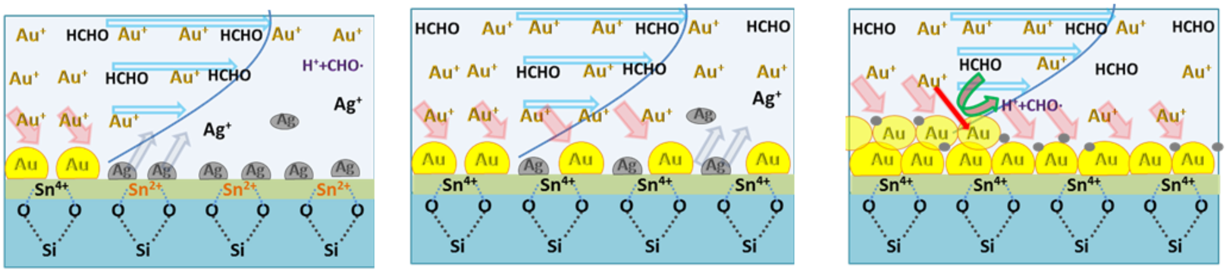

(10) Gal. displacement (11) Transitory Au/Ag alloy* (12) Au deposition

Scheme. S1 Novel physicochemical electroless deposition mechanism

1. Detailed charging correction of XPS results to obtain corrected values as shown in Fig. 6

Reduced Au ions appear to form bulk Au grains at interface and internal structure as deposited EL thin films. Application of XPS to characterize EL Au deposition suggests deposited EL Au exists as bulk grains (> 4 nm) at the interface accompanied by various internal structures. Electron microscopic images show that EL deposition at intermediate times forms Au bulk grains with ~50 nm diameter on the film surface. Fig. 6(A) shows spectra of Au in CF-3-10 film at sputtering time intervals between 0 and 140 sec. The bulk Au in the Au 4f level exhibits two photoemission peaks, $4f_{7/2}$ (84.0 ± 0.2 eV) and $4f_{5/2}$ (87.65 ± 0.2 eV), with intensity ratio of 4:3 and energy difference, the spin-orbit splitting, of 3.65 eV.[1] When the uncorrected raw data from which Fig. 6(A) was obtained were corrected for charging effects using the peak from carbon contamination at the surface, an Au photoemission peak at the surface for 0 min sputtering of 83.7 eV was obtained.(See Table S1) This indicates as-deposited EL Au thin film forms a bulk elemental Au-Au bond at the surface. It also suggests that Au ions deposited by EL Au plating form bulk Au grains with larger than 4 nm diameter, since large metal clusters whose diameters exceed 4 nm have BE values that closely approximate the bulk metal value.[2] When the size of deposited Au cluster decreases to less than 2 nm, the observed core-level Au $4f_{7/2}$ BE increases by a maximum of 0.8 – 1.2 eV. This increase is attributed to effects of decreased core-hole screening by the conduction band, as a result of the discretization of the conduction band.[3,4,5] The SEM images of four different EL Au films (Fig. S5) also confirm that the grain size of deposited Au NPs is larger than ~50 nm. This reaffirms the observed Au peak is the $4f_{7/2}$ Au-Au bulk peak (~84.0 eV) and validates spectral corrections for charging effects.

The observed $Au4f_{7/2}$ peak positions below the surface (0 sec) were also corrected to the referential Au-Au bulk values (~84.0 eV). For CF-3-10 in Fig 6(A), the $Au4f_{7/2}$ peak intensity increased dramatically after the first sputtering, reaching a maximum between 20 and 60 sec, and decreasing at ≥ 80 sec. The intensity increase was attributable to removal of contamination layers associated with disappearance of the carbon peak during the first 20-sec interval of Ar^+ sputtering. Values of FWHM for 20, 40, 60 and 80 sec were 0.76, 0.76, 0.77 and 0.77, respectively. Consistency of the peak intensity and FWHM values indicates the uniformity of reduced metallic Au grains that form the internal structure of CF-EL Au film. The Ar^+ sputtering rate for Au depth profiling was 0.3 ~ 0.7 nm/sec. While bombardment with Ar^+ ions can promote Au diffusion and aggregation and transform Au-Au cluster to Au-Au bulk due to transfer of kinetic energy of the ion to the surface atom,[2] the consistency of the spectral features suggest the bulk elemental Au-Au bond is inherent to the film itself.

Table S1. Peak position of XPS analysis for CF-3-10. The number in bracket is the corrected value after considering charging effect via Au reference.

Sput. Time (sec.)	C1s (C = 284.3~ 285.0)	O1s (SiO$_2$ = 532.5 -533.3)	Si2p (SiO$_2$ = 103.2~ 103.8)	Au 4f$_{7/2}$ (Au= 83.8 ~84.2)	AuSn4 (~85.0)	Ag3d$_{5/2}$ (Ag= 368.1~ 368.3)	Sn3d$_{5/2}$ (SnO$_2$ = 486.5~ 486.9)	Na Auger KLL (~498.0)	Shifting by Au ref (84.0)	Structure
0	284.0 (285.7)	531.1 (532.8)	-	82.3 (84.0)	-	366.1 (367.8)	-	-	+1.7	Surface
20	-	-	-	82.9 (84.0)	-	366.9 (368.0)	-	-	+1.1	Internal (Au)
40	-	-	-	83.0 (84.0)	-	367.1 (368.1)	-	-	+1.0	Internal (Au)
60	-	-	-	83.1 (84.0)	-	367.1 (368.0)	485.9 (486.8)	-	+0.9	Internal (Au)
80	-	531.9/530.7 (532.8/531.6)	-	83.1 (84.0)	-	367.1 (368.0)	485.9 (486.8)	-	+0.9	Internal (Au)
100	-	533.4/530.9 (533.0/530.5)	104.1 (103.7)	84.4 (84.0)	85.4 (85.0)	-	487.4 (487.0)	-	-0.4	Interface
120	-	532.4/529.9 (532.7/530.2)	103.1 (103.4)	83.7 (84.0)	84.7 (85.0)	-	486.5 (486.8)	498.1 (498.4)	+0.3	Interface
140		532.2/530.2 (532.6/530.6)	102.9 (103.3)	83.6 (84.0)	-	-	486.1 (486.5)	497.1 (497.5)	+0.4	Glass

2. Depth profile of XPS peaks for main chemical components of other samples

EL films deposited at other conditions (CF-3-5, BI-5 and BI-10) show comparable XPS composition trends with minor differences. In order to evaluate hydraulic effect on EL plating, other EL films were fabricated by a method of dynamic Au deposition, other words, batch immersion (BI) plating. The procedure was followed by. A Ag-activated substrate was prepared following the procedure outlined for CF-EL deposition in experimental section. Then the unsteady EL Au deposition was performed in the scalable CF-EL plating system by manual, instantaneous mixture of 0.5 ml-total mixture of Au(I) and reducing agent solution followed by injection for one second into the H_2O-filled Ag-activated substrate. A desired batch incubation period, 5 min or 10 min, followed. These samples were designated BI-5 and BI-10 based on the incubation time. After incubation, the deposited Au solution was immediately washed out by subsequent H_2O injection.

The Au4f spectrum of CF-3-5 (Fig. S1(A)) shows another new small peak (~86.4 eV) at 80 sec of depth profile including a shoulder peak of Au-Sn alloy (~85.0 eV). The small peak at 86.4 eV can be tentatively attributed to a non-hydrated Au-oxide compound (~86.3 eV)[2] which is located in the interface of Au film and glass substrate. Besides this peak in the Au4f spectrum, other components in CF-3-5 exhibit compositions similar to CF-3-10 during depth profiling: AgO_x at the surface, elemental Ag across the internal Au film, and Au-Sn alloy and SnO_2 at the silica-metal interface along with appearance of Na and Si peaks. Fig. S2 shows in the 5-min batch immersion sample, BI-5, metal components disappeared from XPS spectra at earlier intervals (40~60 sec), corresponding to lower mass transfer rate, shorter deposition time, and therefore less deposited mass compared to CF-3-10 or BI-10. The 10-min batch immersion sample, BI-10, as shown in Fig. S3, exhibited less Sn content than other EL-films. The Sn3d peak occurred at lower intensity and the shoulder peak of Au-Sn alloy in the spectrum of Au4f was not detected at the interface between Au film and glass substrate. Besides the low Sn content, other spectral features at the film surface, internal structures, and interface with the glass substrate were similar to features of CF-3-10, suggesting comparable compositional topography.

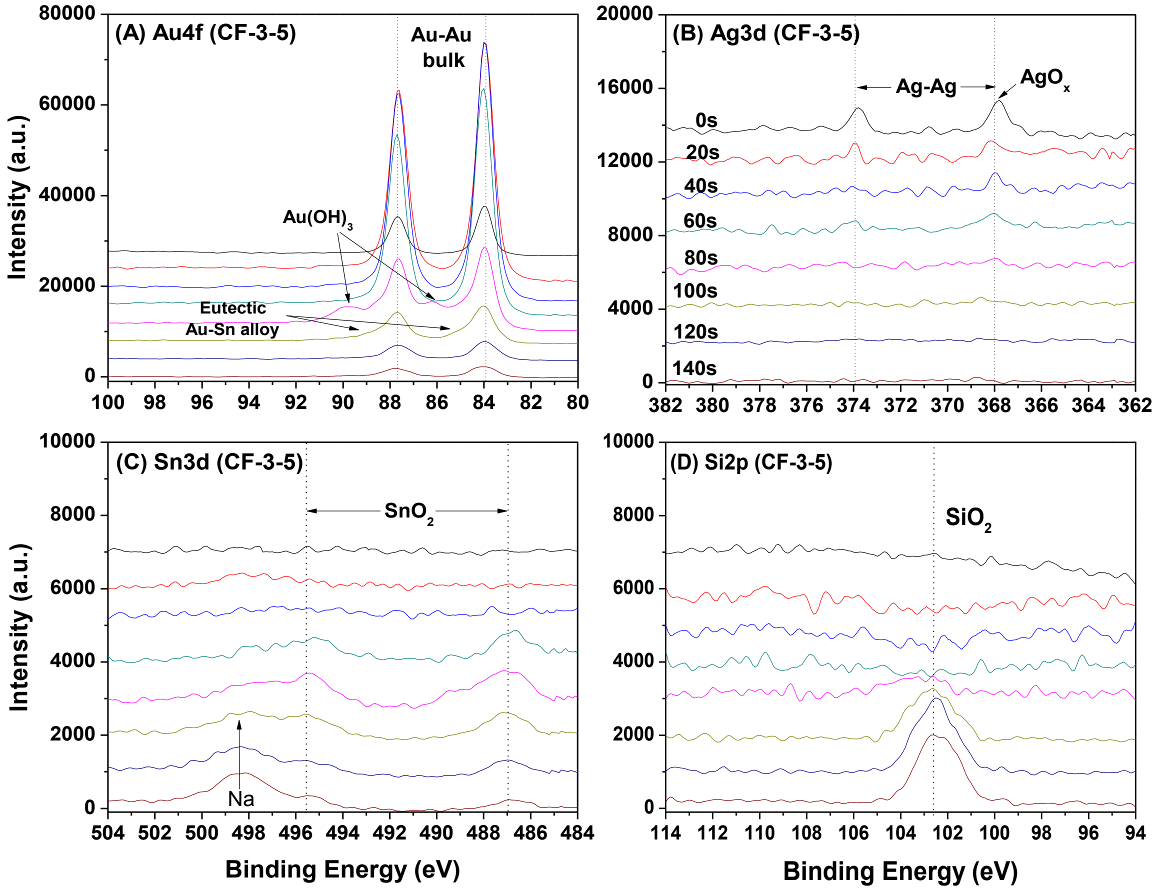

Fig. S1 The XPS depth profiles of CF-3-5 for main chemical components: (A) Au4f; (B) Ag3d; (C) Sn3d; (D) Si2p

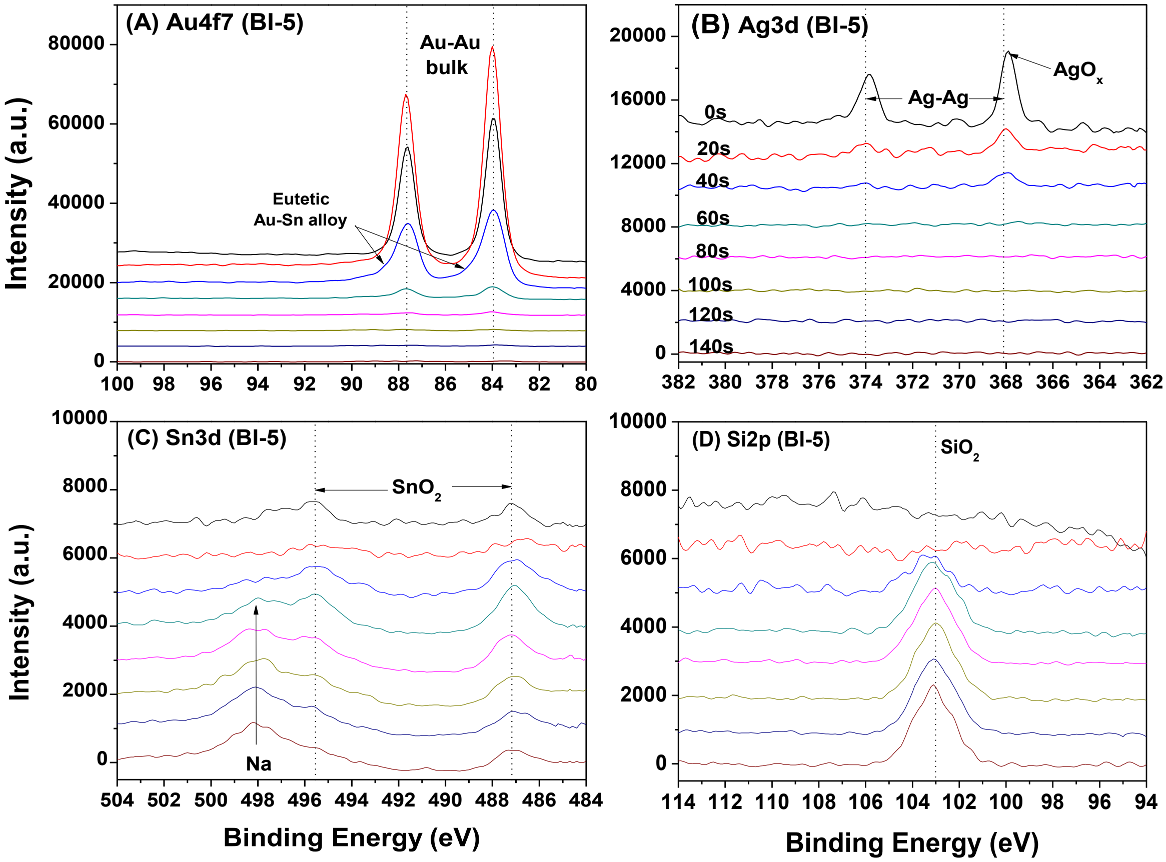

Fig. S2 The XPS depth profiles of BI-5 for main chemical components: (A) Au4f; (B) Ag3d; (C) Sn3d; (D) Si2p

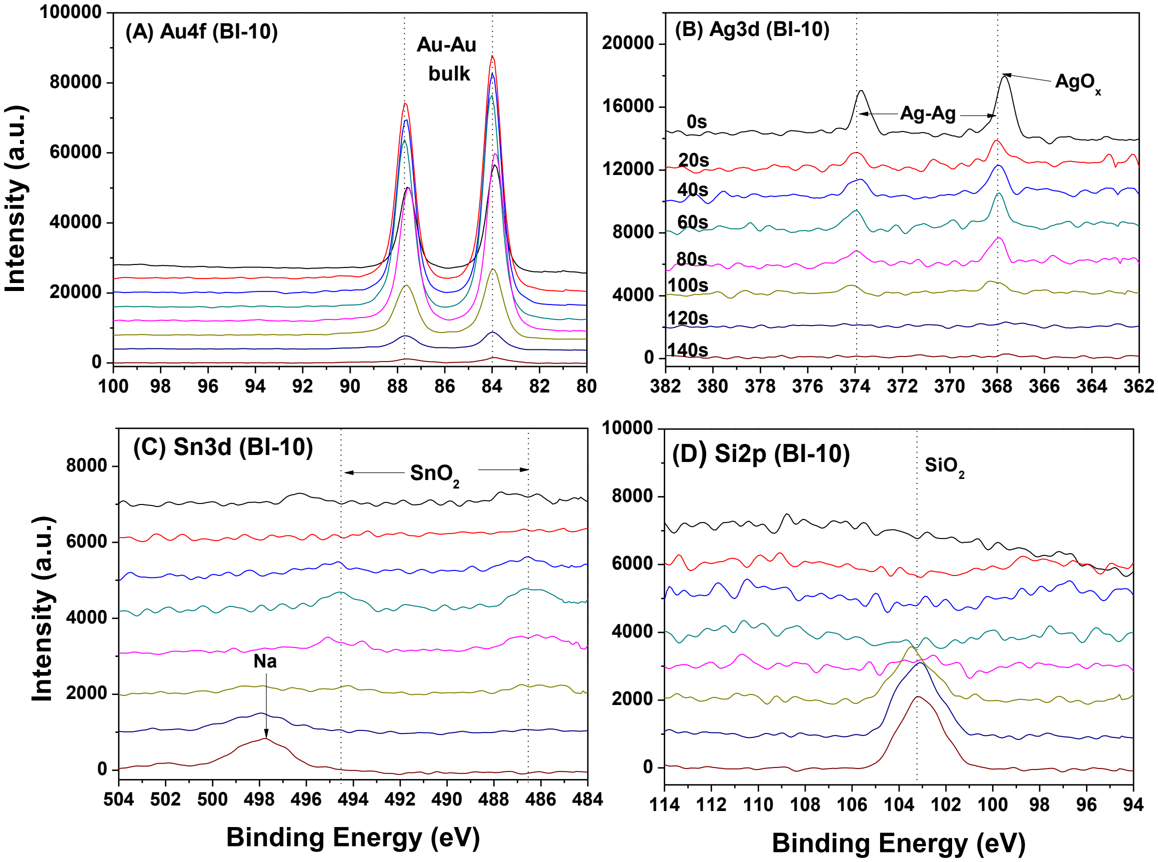

Fig. S3 The XPS depth profiles of BI-10 for main chemical components: (A) Au4f; (B) Ag3d; (C) Sn3d; (D) Si2p

3. Quantitative XPS analysis allows identification of hydraulic and spatiotemporal effects during EL deposition.

Fig. S4 compares the quantitative atomic % composition of CF- and BI-EL film during intermittent 20 sec depth profiling for total 150 sec. For CF-3-5, as shown in Figure S4(A), at the surface (0 sec sputtering), the Au content is ~15.2 % due to organic carbonate contamination and silver oxide particle residue, 50.2% of C and 24.8% of O, 1.6% of Ag. After 20 sec sputtering, the Au concentration dramatically increased to 83.7 % whereas C and O contents decrease to 9.9 and 4.1%, respectively. The further 40 sec sputtering exhibit improved Au content to 89.7 % with further decreased 5.5% of C and 3.5 % of O, which represent the chemical composition of internal structure of EL Au film. After 60 sec, the Au content decrease to 81.5% due to increasing 7.9% of oxygen content which may be mainly originated from metal oxides such as Au, Ag (0.8%) and Sn (3.4%). The Sn content was suddenly increased from 0.3 % of 40 sec of sputtering. No Si was detected at this sputtering step. At 80 sec, the Au content decrease to 44.7 %, while O, Si and Sn increase 34.0%, 10.4% and 4.6%, respectively. After 100 sec, the content of O (59.5%) and Si (20.4%) exceed Au content (14.6%). Interestingly, the Sn content deceases to 2.5 %. Based on this observation, the interface of CF-3-5 film may be revealed after 80~100 sec of Ar sputtering. The interface area is indicated by dot box in Fig. S4(C). After 120 sec, the O, Si, and Na content are stabilized in 64.4 ± 0.9%, 27.3 ± 0.2%, and 2.3 ± 0.3% to 240 second. These three main components are contributed to soda lime silica glass substrate.

The content of O throughout the Au film may indicate metal oxide formation during EL Au plating. Generally, the mole ratio of O to Si from silicate glass substrate is 2.36 ± 0.03, resulting from observation during 140 ~ 240 second depth profile. The depth profile after 140 sec was omitted in Fig. S4 for clarity. During 20 ~ 100 seconds, ∞ (no Si), ∞,∞, 3.3 and 2.97 of the mole ratio which exceed 2.36 of silicate (SiO_2) represent the existence of metal oxides such as SnO_2, AuO_x and AgO_x. For CF-3-10, 80 and 100 second of depth profile also show 9.16 and 2.97 of mole ratio (O/Si) with larger than 2.48±0.14 which is from depth profile of glass after 140 sec. For BI-5, 20 and 40 second of depth profile also show 2.89 and 2.60 of mole ratio (O/Si) with larger than 2.41±0.07. For BI-10, 60 and 80 second of depth profile also show 2.89 and 2.60 of mole ratio (O/Si) with larger than 2.41±0.07.

Other EL film's atomic concentration profile also exhibit similar pattern for distinguishable structural features such as surface, internal structure of Au film, interface and SiO_2 substrate. However, the interface locations or film thickness are dependent on different Au mass transferred amount induced by varying deposition time and hydrodynamic conditions. Considering main components distribution, Au, O and Si, the location of interface composition was assigned to below 10% of Au and more than 30% and 15% of O and Si. Based on this standard the interface of BI-5, BI-10, CF-3-5 and CF-3-10 are assigned to ~55, ~100, ~110 and ~130 sec. The hydrodynamic comparison clearly shows that the thickness of CF-EL films is higher than BI-EL films at the same deposition time. The increased mass transfer rate and steady higher average local concentration during CF increase the deposited amount relative to batch immersion, resulting in thicker films.

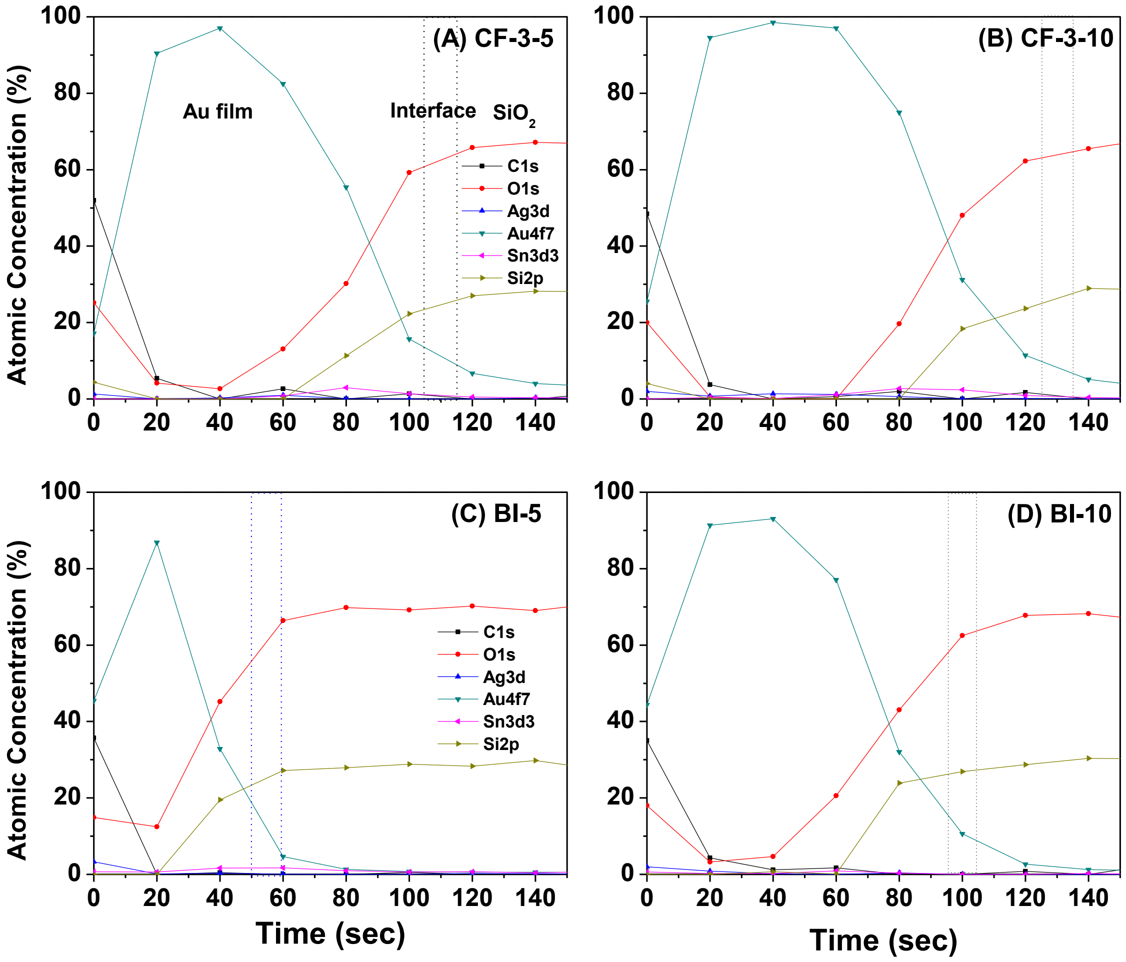

Fig. S4 Quantitative chemical component characterization of XPS depth profile of two different CF and BI deposited film for 5 and 10 min. Target chemical components are C1s, O1s, Ag3d, Au4f7, Sn3d3 and Si2P.

4. SEM image of EL Au films

Intermediate deposition times produce continuous deposited film with packed uniform grains**.** Steady diffusion in equilibrium hydraulic conditions (i.e. CF) has been shown to produce EL Au films at short deposition times that exhibit more uniform surface morphology and optical features than EL films formed by unsteady-state diffusion in batch immersion (i.e. BI), or by vacuum vapor-deposited films.[6] For deposition times in the range of 20 sec, 60 sec and 4 min, BI-EL plating yields discrete nucleated Au NPs, separated island, and discontinuous island films on quartz slides, respectively.[7] Without surface pretreatment and conductive substrate, vapor deposition usually produces separate island thin film structure due to lattice mismatch. Equilibrium, steady diffusion via a constant concentration driving force in CF-EL plating improves continuity and uniformity of EL film for 2 min deposition relative to BI-EL film for 2 min.[6] The steady, higher mass transfer rate improved the surface morphology and uniformity, however the effect of extended plating time and different hydraulic conditions on film thickness and surface morphology have not been investigated for CF-EL thin films.

In this work, EL Au thin films were produced at longer deposition times of 5 min and 10 min, respectively, at both unsteady and steady hydrodynamic conditions. For 5 min BI deposition time, the EL Au film, as shown in SEM image of Fig. S5(C), exhibit uniformly close packed grain structures with less than 50 nm diameter. Increasing BI deposition time to 10 min (BI-10) and performing continuous, equilibrium deposition at similar hydraulic conditions of about 3 mL/hr (CF-3-5, CF-3-10) also exhibit very similar close packed grain structure. It appears that the HCHO driven autocatalytic Au reduction on nucleated Au NPs form uniform Au grains during intermediate deposition. Measurement of surface roughness for these intermediate deposition times is the subject of future work.

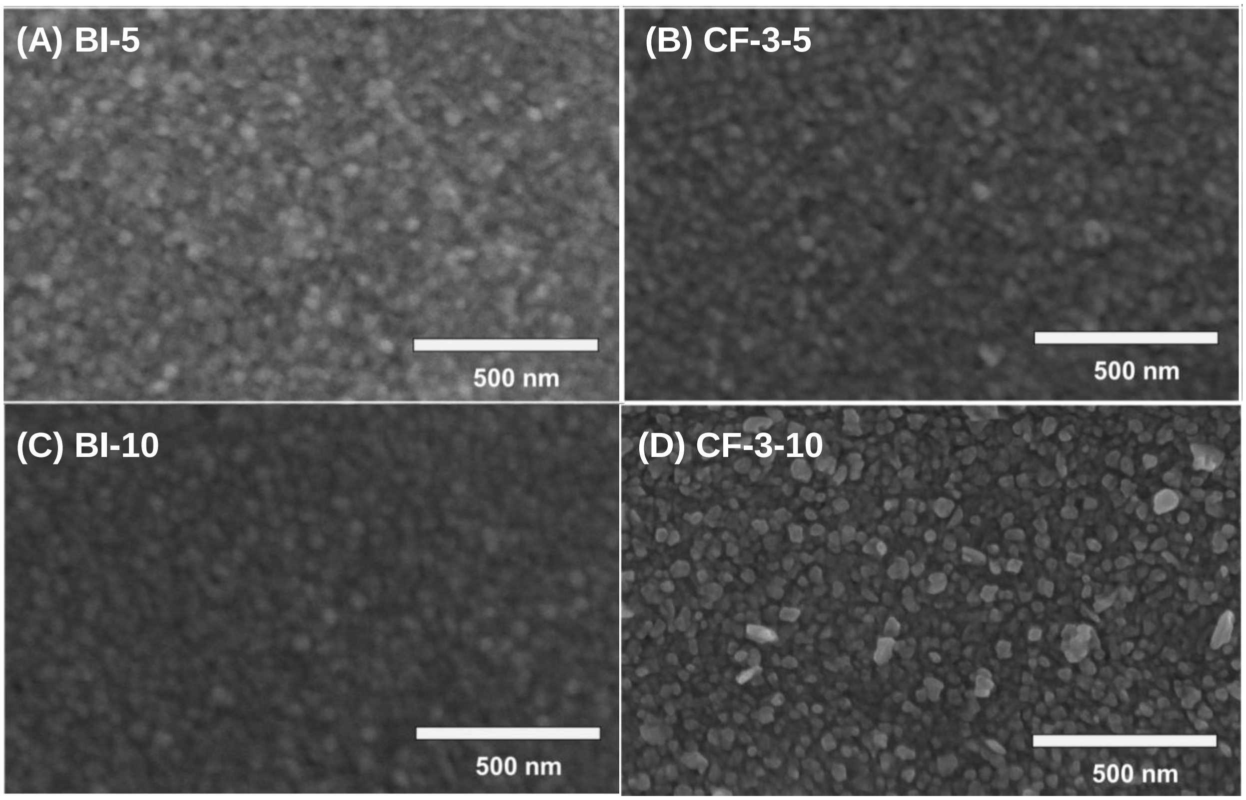

Fig. S5 SEM images of EL Au films: A) BI-5 B) CF-3-5 C) BI-10 D) CF-3-10.

Reference

---

(1) C. D. Wagner, W. M. Riggs, L. E. Davis, J. F. Moulder, G. E. Muilenberg, in Handbook of X-ray photoelectron Spectroscopy, Perkin-Elmer Corporation, Minnesota, 1978

(2) N. M. Figueiredo, N. J. M. Carvalho, and A. Cavaleiro, *Appl. Surf. Sci.*, 2011, ***257***, 5793.

(3) C. N. R. Rao, V. Vijayakrishnan, H. N. Aiyer, G. N. Kulkarni and G. N. Subbanna, *J. Phys, Chem*. 1993, ***97***, 11157.

(4) M. G. Mason, *Phys, Rev. B*, 1983, ***27***, 748.

(5) T. T. Magkoev, K. Christmann, A. M. C. Moutinho and Y. Murata, *Surf. Sci.*, 2002, ***515***, 538.

(6) G. G. Jang and D. K. Roper, *J. Phys. Chem. C*, 2009, ***113***, 19228.
(7) W. Ahn, B. Taylor, A. G. Dall'Asén and D. K. Roper, *Langmuir*, 2008, ***24***, 4174-4184.